Simultaneously Transmitting And Reflecting RIS Aided NOMA With Randomly Deployed Users

Chao Zhang, Wenqiang Yi, Kaifeng Han, Yuanwei Liu, Zhiguo Ding, Marco Di Renzo

Simultaneously Transmitting And Reflecting RIS Aided NOMA With Randomly Deployed Users

Chao Zhang*, Wenqiang Yi*, Kaifeng Han†, Yuanwei Liu*, Zhiguo Ding‡ and Marco Di Renzo§
*Queen Mary University of London, London, UK
†China Academy of Information and Communications Technology, China
‡The University of Manchester, Manchester, UK
§Université Paris-Saclay and CNRS, Gif-sur-Yvette, France

***Abstract*—To achieve 360° coverage, we investigate a simultaneous transmitting and reflecting reconfigurable intelligent surfaces (STAR-RIS) aided downlink non-orthogonal multiple access (NOMA) network with randomly deployed users. For different scenarios, we first derive two STAR-RIS-aided channel models, namely the central limit model and the curve fitting model. More specifically, the central limit model fits the scenarios with numerous RIS elements while the curve fitting model can be extended to multi-cell scenarios. The analytical results reveal that 1) the central limit model has closed-form expressions calculated as the error functions, and 2) the curve fitting model can be closely modeled as a Gamma distribution. We then derive the closed-form outage probability expressions for the NOMA users. Numerical results indicate that 1) the two channel models match the simulation results well in low signal-to-noise-ratio (SNR) regions and perform as boundaries in high SNR regions, 2) the central limit model performs as an upper bound of the simulation results, while a lower bound can be obtained by the curve fitting model, and 3) the both users in the NOMA pair have no error floor.**

I. Introduction

As a promising technique of the six-generation of wireless communications (6G) [1], [2], reconfigurable intelligent surfaces (RIS) can enhance the channel quality of the current networks. However, a key challenge is posed that the substrates of RISs are always opaque items that may block the signals to the users behind RISs. As a solution, the recent development of meta-surfaces, namely the simultaneous transmitting and reflecting reconfigurable intelligent surfaces (STAR-RIS), allows signals through the RISs via refraction. Hence, independent reflection and refraction beamforming techniques allow high flexibility of RIS serving areas, which is enhanced from a half circle to a whole circle area [3].

The recent research focuses on the optimal beamforming designs of STAR-RIS networks based on power consumption minimization [4], phase shift optimization [5], and sum-rate maximization [6], while theoretical performance analysis is still in their infancy. Additionally, STAR-RISs can artificially allocate different radiation power levels of the received signals to the reflecting and transmitting users, which improves the flexibility for downlink non-orthogonal multiple access (NOMA) networks [7]. In this way, STAR-RISs can adjust and distinguish the power levels of users to maintain the constraint of successive interference cancellation (SIC), which may enhance the success rate of the SIC process in NOMA networks. Hence, the benefits of STAR-RISs to NOMA networks are highly valuable to be investigated.

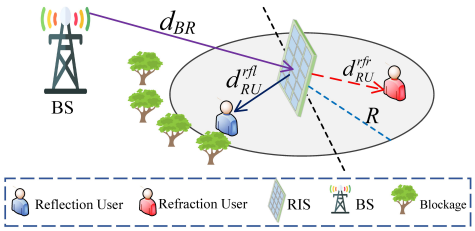

Fig. 1. System model

Motivated by the aforementioned advantages, we investigate a STAR-RIS-aided downlink NOMA network to analyze the outage performance. The main contributions can be summarized as follows. We first derive two STAR-RIS-aided channel models, namely the central limit model and the curve fitting model. Based on the two channel models, we additionally derive the closed-form expressions of outage probability for the transmitting and reflecting users. Finally, numerical results illustrate that 1) increasing the RIS elements can enhance the performance of NOMA users, 2) STAR-RISs increase the serving area of users, and 3) our channel models match simulation results well in low signal-to-noise-ratio (SNR) regions and perform as close boundaries in high SNR regions.

II. System Model

A STAR-RIS-aided downlink NOMA network is considered, which includes a fixed base station (BS), fixed STAR-RISs, and randomly deployed users (reflecting and transmitting users). We consider a reflecting user and a transmitting user are paired in the same resource block with different power levels. The direct links from the BS to the reflecting user are assumed as a blocked scenario. More specifically, the direct link to the reflecting user is blocked by an obstacle, such as trees or buildings. We note that STAR-RISs are transparent for the signals of the transmitting user. The links from the BS to the transmitting user pass through the RISs by refraction, denoted as the transmitting links. Hence, the BS firstly transmits signals to the RISs, followed by the radiation signals to the reflecting user and the transmitting user.

A. Theoretic Foundation of STAR-RIS

We define the reflecting and transmitting coefficients as R_m and T_m for the m^{th} RIS element, respectively. We consider

that the phase shift coefficients ϕ_m^{rfl} and ϕ_m^{rfr} are two independent variables for the reflecting user and transmitting user, respectively. Additionally, we assume the STAR-RIS has M elements satisfying $1 \leq m \leq M$. Hence, the reflected and refracted signals of the m^{th} RIS element can be expressed as $R_m = \sqrt{\beta_m^{rfl}} e^{j\phi_m^{rfl}}$ and $T_m = \sqrt{\beta_m^{rfr}} e^{j\phi_m^{rfr}}$, respectively, where $\phi_m^{rfl}, \phi_m^{rfr} \in [0, 2\pi)$. Additionally, the β_m^{rfl} is the energy splitting coefficient for reflecting links and the β_m^{rfr} the energy splitting coefficient for transmitting links.

We exploit the energy splitting (ES) protocol in this paper [4]. In terms of the ES protocol, we consider all the RIS elements (M elements) can simultaneously operate refracting and reflecting modes, while the total radiation energy is split into two parts. When assuming the STAR-RISs are passive with ignorable energy consumption, we can present a constraint on the aforementioned coefficients as $|R_m|^2 + |T_m|^2 \leq 1$. Hence, we can mathematically present this protocol as $\beta_m^{rfl} + \beta_m^{rfr} \leq 1$ [3], where $\beta_m^{rfl}, \beta_m^{rfr} \in (0, 1)$. As we expect the best utilization rate of RIS elements, we assume $\beta_m^{rfl} + \beta_m^{rfr} = 1$ in the following investigation.

B. Deployment of Devices

We consider a single-cell STAR-RIS-aided NOMA network. In this case, the BS is deployed at the center of the cell. As RISs are always deployed at buildings facades, the positions of RISs are fixed and known. We choose one of them to investigate the performance with its position $\mathbf{x_R}$. As we assume the RISs are deployed on tall buildings, the links between the BS and the RIS elements are line of sight (LoS) links. For the users, the positions of the reflecting user and the transmitting user are expressed as $\mathbf{x_{rfl}}$ and $\mathbf{x_{rfr}}$, respectively. Hence, we define the channel links as three types: 1) the links between the BS and the RIS as BR links with the distance $d_{BR} = \|\mathbf{x_R}\|$, 2) the links between the RIS and the reflecting user as RU_{rfl} links with the distance $d_{RU}^{rfl} = \|\mathbf{x_R} - \mathbf{x_{rfl}}\|$, and 3) the links from the RIS to the transmitting user as RU_{rfr} links with the distance $d_{RU}^{rfr} = \|\mathbf{x_R} - \mathbf{x_{rfr}}\|$.

We exploit a homogeneous Poisson point processes (HPPP) to mimic the distribution of users, namely $\Phi_u \subset \mathbb{R}^2$ with density λ_u. Hence, we obtain that users are uniformly distributed within the serving area of the RIS. Without loss of generality, we consider the serving area of the RIS is a circle with the radius R, denoted as $\mathbb{O}(0, R)$, where $\mathbb{O}(a, b)$ is an annulus with the inner radius a and outer radius b. Additionally, this area is split into two parts: 1) the half ball facing the RIS as the reflecting area, namely $\mathbb{B}_{rfl}$, and 2) the rest half ball behind of the RIS as the refracting area, namely $\mathbb{B}_{rfr}$. We randomly choose a user from $\mathbb{B}_{rfl}$ and a user from $\mathbb{B}_{rfr}$ as the NOMA pair. Hence, we can evaluate the spatial effects of users by investigating the chosen NOMA pair via stochastic geometry methods. In this case, the probability density functions (PDFs) of d_{RU}^{rfl} and d_{RU}^{rfr} are expressed as

$$f_{d_{RU}^{rfl}}(x) = f_{d_{RU}^{rfr}}(x) = \frac{\partial}{\partial x} \int_0^{\pi} \int_0^{x} \frac{2r}{\pi R^2} dr d\theta = \frac{2x}{R^2}. \quad (1)$$

C. Signal Model

Based on the NOMA technique, the strong NOMA user in the NOMA pair accomplishes the successive interference cancellation (SIC) procedure. In this model, as the RIS can adjust the energy splitting coefficients β_m^{rfl} and β_m^{rfr}, we can artificially allocate more energy for reflecting links. In practical scenarios, to maintain the links between the RIS and the users are LoS links, we assume the radius of RIS serving area R is not large. Thus, the influence of path loss is not severe. Under this situation, we can find a pair of energy allocation coefficients (β_m^{rfl} and β_m^{rfr}) by the RIS to maintain that the reflecting user always keeps as the strong user. Therefore, the reflecting user will take over the SIC process. Based on this assumption, the channel models are designed in the following.

1) Small-Scale Fading Model: We assume that all the links follow the Rician distribution. We denote the small-scale fading of three types of links as $h_{BR,m}$ for BR links, $h_{RU,m}^{rfl}$ for RU_{rfl} links, and $h_{RU,m}^{rfr}$ for RU_{rfr} links for $\forall m \in \{1, 2, \cdots, M\}$. Hence, the PDF for Rician distribution can be expressed as

$$\begin{aligned} &f_{h_{BR,m}}(x) = f_{h_{RU,m}^{rfl}}(x) = f_{h_{RU,m}^{rfr}}(x) \\ &= \frac{2(1+k_m)}{\exp(k_m)} x \exp\left[-(1+k_m)x^2\right] I_0\left[2\sqrt{k_m(1+k_m)}x\right], \quad (2) \end{aligned}$$

where k_m is the coefficient of Rician distribution and $I_0(x)$ is the Bessel function. In this case, we assume that the mean values and variances of all the Rician channels are the same, denoted as $\bar{h} = \sqrt{\frac{\pi}{4(1+k)}} {}_1F_1\left(-\frac{1}{2}, 1; -k\right)$ and $\eta = 1 - \frac{\pi}{4(1+k)}\left[{}_1F_1\left(-\frac{1}{2}, 1; -k\right)\right]^2$, where ${}_1F_1(\cdot,\cdot;\cdot)$ is the confluent hypergeometric function of the first kind.

We combine the BR and RU_{rfl} links as the reflecting links, namely g_m^{rfl} for the m^{th} RIS element. Additionally, we combine the BR and RU_{rfr} links as the transmitting links, namely g_m^{rfr} for the m^{th} RIS element. Based on the theoretic fundamental constraint of STAR-RISs, we express the small-scale fading model of the reflecting and transmitting links as

$$\left|g_m^{rfl}\right| = \left|\mathbf{G_{RU}^{rfl}} \mathbf{\Theta_{rfl}} \mathbf{G_{BR}}\right|, \left|g_m^{rfr}\right| = \left|\mathbf{G_{RU}^{rfr}} \mathbf{\Theta_{rfr}} \mathbf{G_{BR}}\right|, \quad (3)$$

where $\mathbf{\Theta_{rfl}} = \mathrm{diag}[\sqrt{\beta_1^{\mathrm{rfl}}} \mathrm{e}^{\mathrm{j}\phi_1^{\mathrm{rfl}}}, \sqrt{\beta_2^{\mathrm{rfl}}} \mathrm{e}^{\mathrm{j}\phi_2^{\mathrm{rfl}}}, \cdots, \sqrt{\beta_{\mathrm{M}}^{\mathrm{rfl}}} \mathrm{e}^{\mathrm{j}\phi_{\mathrm{M}}^{\mathrm{rfl}}}]$ is the diagonal matrix for reflecting links, $\mathbf{\Theta_{rfr}} = \mathrm{diag}[\sqrt{\beta_1^{\mathrm{rfr}}} \mathrm{e}^{\mathrm{j}\phi_1^{\mathrm{rfr}}}, \sqrt{\beta_2^{\mathrm{rfr}}} \mathrm{e}^{\mathrm{j}\phi_2^{\mathrm{rfr}}}, \cdots, \sqrt{\beta_{\mathrm{M}}^{\mathrm{rfr}}} \mathrm{e}^{\mathrm{j}\phi_{\mathrm{M}}^{\mathrm{rfr}}}]$ is the diagonal matrix for transmitting links, $\mathbf{G_{RU}^{rfl}} = [h_{RU,1}^{rfl}, h_{RU,2}^{rfl}, \cdots, h_{RU,M}^{rfl}]^T$ is the small-scale fading of the reflecting links, $\mathbf{G_{RU}^{rfr}} = [h_{RU,1}^{rfr}, h_{RU,2}^{rfr}, \cdots, h_{RU,M}^{rfr}]^T$ is the small-scale fading for the transmitting links, and $\mathbf{G_{BR}} = [h_{BR,1}, h_{BR,2}, \cdots, h_{BR,M}]$ is the small-scale fading of BR links.

2) STAR-RIS-Aided Path Loss Model: We define the path loss model of the three links via conventional wireless communication models. Hence, we can respectively express the path

loss expressions for BR, RU_{rfl}, and RU_{rfr} links as

$$\mathcal{P}_{BR}(\mathbf{x}_R)=C_{BR}\|\mathbf{x_R}\|^{-\alpha_t}=C_{BR}d_{BR}^{-\alpha_t}, \tag{4}$$

$$\mathcal{P}_{RU}^{rfl}(\mathbf{x}_R,\mathbf{x_{RU}^{rfl}})=C_{RU}^{rfl}\left\|\mathbf{x}_R-\mathbf{x_{RU}^{rfl}}\right\|^{-\alpha_t}=C_{RU}^{rfl}\left(d_{RU}^{rfl}\right)^{-\alpha_t}, \tag{5}$$

$$\mathcal{P}_{RU}^{rfr}(\mathbf{x_R},\mathbf{x_{RU}^{rfr}})=C_{RU}^{rfr}\left\|\mathbf{x}_R-\mathbf{x_{RU}^{rfr}}\right\|^{-\alpha_t}=C_{RU}^{rfr}\left(d_{RU}^{rfr}\right)^{-\alpha_t}, \tag{6}$$

where the $\mathcal{P}$ expresses the path loss, $\{C_{BR},C_{RU}^{rfl},C_{RU}^{rfr}\}=\left(\frac{c}{4\pi f_c}\right)^2$ are reference-distance-based intercepts for different links and the reference distance $d_0=1$ m in this work, where $c=3\times10^8$ m/s is the speed of light and f_c is the carrier frequency. The α_t is the path loss exponent for users.

3) Signal-to-Interference-and-Noise Ratio (SINR): To maintain the strong user (the reflecting user) with SIC process, we allocate more power to the week user (the transmitting user) in NOMA pair. Hence, the SINR of the SIC process for the reflecting user is given by

$$\gamma_{\mathrm{SIC}}=\frac{a_{rfr}P_t\mathcal{P}_{BR}(\mathbf{x}_R)\mathcal{P}_{RU}^{rfl}(\mathbf{x}_R,\mathbf{x}_{RU}^{rfl})\left|g_m^{rfl}\right|^2}{a_{rfl}P_t\mathcal{P}_{BR}(\mathbf{x}_R)\mathcal{P}_{RU}^{rfl}(\mathbf{x}_R,\mathbf{x}_{RU}^{rfl})\left|g_m^{rfl}\right|^2+\sigma^2}, \tag{7}$$

where P_t is the transmit power, σ^2 is the variance of additive white Gaussian noise (AWGN), and a_{rfr} and a_{rfl} are power allocation coefficients with $a_{rfr}+a_{rfl}=1$ and $a_{rfl}<a_{rfr}$.

With the aid of the SIC process, the reflecting user can remove the messages of the transmitting user. Then, the reflecting user can decode its required messages. Hence, the signal-to-noise ratio (SNR) of the reflecting user can be presented as

$$\gamma_{\mathrm{rfl}}=\frac{a_{rfl}P_t\mathcal{P}_{BR}(\mathbf{x}_R)\mathcal{P}_{RU}^{rfl}(\mathbf{x}_R,\mathbf{x}_{RU}^{rfl})\left|g_m^{rfl}\right|^2}{\sigma^2}. \tag{8}$$

When we consider the other NOMA user's messages as interference, the transmitting user can directly decode its signal. Hence, the SINR of the transmitting user is expressed as

$$\gamma_{\mathrm{rfr}}=\frac{a_{rfr}P_t\mathcal{P}_{BR}(\mathbf{x}_R)\mathcal{P}_{RU}^{rfr}(\mathbf{x}_R,\mathbf{x}_{RU}^{rfr})\left|g_m^{rfr}\right|^2}{a_{rfl}P_t\mathcal{P}_{BR}(\mathbf{x}_R)\mathcal{P}_{RU}^{rfr}(\mathbf{x}_R,\mathbf{x}_{RU}^{rfr})\left|g_m^{rfr}\right|^2+\sigma^2}. \tag{9}$$

Based on the aforementioned SINR expressions, we can firstly derive the STAR-RIS-aided channel models in the following.

III. STAR-RIS-aided Channel Model

One of the challenges for STAR-RIS-aided networks is to derive tractable mathematical channel models. Hence, we present two mathematical models in different application scenarios, namely the central limit model and the curve fitting model. More specifically, the central limit model is suitable for large RISs with a large number of elements, while the curve fitting model can fit all scenarios. Detailed derivations and discussions are expressed as follows.

A. Central Limit Model

When we assume the channel gains of all the elements of RISs are irrelevant, the channel model of RIS-aided networks can be expressed as the summation of different variables. Hence, the central limit theorem is an appropriate mathematical tool to derive the approximated channel model. Although it has the constraint that the RIS elements are large enough, the central limit model is one of the most popular models in recent works because of its great tractability on derivations. Hence, under the case with quantities of uncorrelated channels passing by different RIS elements, we can exploit the central limit model to investigate the channel performance.

Lemma 1: We assume that the quantity of RIS elements M is large and the channels for different RIS elements are independent. For the ES protocol and with the aid of the central limit theorem, the PDF and cumulative distribution function (CDF) of the central limit model are derived as

$$f_{\left|g_m^{rf}\right|^2}(y)=\frac{1}{2\sqrt{2\pi\eta_{eq}^{rf}}}\frac{1}{\sqrt{y}}\left(\exp\left(-\frac{\left(\sqrt{y}-\bar{h}_{eq}^{rf}\right)^2}{2\eta_{eq}^{rf}}\right)+\exp\left(-\frac{\left(\sqrt{y}+\bar{h}_{eq}^{rf}\right)^2}{2\eta_{eq}^{rf}}\right)\right), \tag{10}$$

$$F_{\left|g_m^{rf}\right|^2}(y)=\frac{1}{2}\left(\mathrm{erf}\left(\frac{\bar{h}_{eq}^{rf}+\sqrt{x}}{\sqrt{2\eta_{eq}^{rf}}}\right)-\mathrm{erf}\left(\frac{\bar{h}_{eq}^{rf}-\sqrt{x}}{\sqrt{2\eta_{eq}^{rf}}}\right)\right), \tag{11}$$

where $\bar{h}_{eq}^{rf}$ is the mean value of $|g_m^{rf}|$ with $rf\in\{rfr,rfl\}$ representing the transmitting links and the reflecting links, respectively. The η_{eq}^{rf} is the variance of $|g_m^{rf}|$. Based on the properties of the expectation and the variance for independent variables, we derive $\bar{h}_{eq}^{rf}=\sqrt{\beta_{rf}}M\bar{h}^2$ and $\eta_{eq}^{rf}=\beta_{rf}M\left(2\bar{h}^2\eta+\eta^2\right)$. Additionally, the function $\mathrm{erf}(\cdot)$ is the error function.

Proof: See Appendix A. ■

B. Curve Fitting Model

Although the central limit model provides closed-form expressions, its constraints cannot be ignored. Firstly, the central limit model cannot match the RIS-aided networks with few elements, thereby we need a channel model for these scenarios. Additionally, we expect that the channel models have exponential functions, which are tractable for multi-cell scenarios as we always use the Laplace transform to calculate the interference.

Based on the two motivations, we exploit the Matlab curve fitting tool to mimic the channel model as an extant distribution. The advantage of the curve fitting model is that it suits all scenarios and tractable for further derivations. Additionally, it can even fit the scenarios when the RIS elements are correlated. However, the curve fitting model does not conclude the detailed mathematical proof by derivations. Moreover, exploring an accurate distribution may be challenging in some specific cases.

In our paper, we consider the channels of different RIS elements are independent Rician distributions. Thus, we can approximately mimic the channel model as a Gamma distribution. As this approximation is not more accurate than the

central limit model, we can harness it as an alternative when utilizing small RIS with few elements or multi-cell scenarios.

Lemma 2: Utilized the curve fitting tool, it indicates that the combined channel gain $\left|g_m^{rf}\right|^2$ can be simulated as the Gamma distribution with the element α and β. Hence, the PDF and CDF for the curve fitting model can be expressed as

$$f_{\left|g_m^{rf}\right|^2}(x) = \frac{x^{\alpha-1}}{\Gamma(\alpha)(\beta_{rf}\beta)^{\alpha}} \exp\left(-\frac{x}{\beta_{rf}\beta}\right), \quad (12)$$

$$F_{\left|g_m^{rf}\right|^2}(x) = \frac{\gamma\left(\alpha, \frac{x}{\beta_{rf}\beta}\right)}{\Gamma(\alpha)}, \quad (13)$$

where $\gamma(\cdot,\cdot)$ is the incomplete Gamma function and $\Gamma(\cdot)$ is the Gamma function. Based on the Matlab curve fitting tools, we obtain the values of two coefficients as $\alpha = M$ and $\beta < M$, e.g., $\alpha = 30$ and $\beta = 22.46$ when the RIS elements $M = 30$. The CDF of curve fitting model is shown in Fig. 2 in the section of Numerical Results.

Proof: As $\left|g_m^{rf}\right|^2 = \beta_{rf}\left(\sum_{m=1}^{M} h_{RU,m}^{rf} h_{BR,m}\right)^2$ with $rf \in \{rfl, rfr\}$ represents the reflecting and transmitting links, we utilize the curve fitting tool to mimic the variable of $\frac{|g_m^{rf}|^2}{\beta_{rf}}$ as a Gamma distribution. Hence, we express the PDF of $\frac{|g_m^{rf}|^2}{\beta_{rf}}$ as

$$f_{\left|g_m^{rfl}\right|^2/\beta_{rf}}(x) = \frac{x^{\alpha-1}}{\Gamma(\alpha)\beta^{\alpha}} \exp\left(-\frac{x}{\beta}\right). \quad (14)$$

Based on (14), we finally derive the final PDF and CDF of $\left|g_m^{rf}\right|^2$ as (12) and (13) in this theorem. ∎

IV. Outage Performance Analysis

In this section, we investigate the outage performance of the STAR-RIS-aided downlink NOMA network. More specifically, we consider exploiting the central limit model and the curve fitting model to calculate the approximated expressions of the outage probability for the reflecting and transmitting users. Based on the NOMA technique, we first express the definition of the outage probabilities of the reflecting and transmitting users as

$$P_{out,rfl}(x) = 1 - \Pr\left\{\gamma_{\text{SIC}} > \gamma_{th}^{SIC}, \gamma_{rfl} > \gamma_{th}^{out}\right\}, \quad (15)$$

$$P_{out,rfr}(x) = \Pr\left\{\gamma_{rfr} < \gamma_{th}^{out}\right\}, \quad (16)$$

where we express the SIC threshold as γ_{th}^{SIC} and the outage threshold as γ_{th}^{out}. We then calculate the closed-form outage probability expressions based on the two aforementioned models as follows.

A. Central Limit Model

As we have calculated the channel model by *Lemma 1*, we first utilize the central limit model to calculate the approximated outage probability expressions of the reflecting and transmitting users. Note that we have defined the power allocation coefficients as a_{rfr} and a_{rfl} for the transmitting user and reflecting user, respectively. Additionally, we express the SIC threshold as γ_{th}^{SIC} and the outage threshold as γ_{th}^{out}. Based on the outage probability definitions, we can obtain that $P_{out,rfl}^{cl}(x) = 1$ when $a_{rfr} < \gamma_{th}^{SIC} a_{rfl}$ and $P_{out,rfr}^{cl}(x) = 1$ when $a_{rfr} < \gamma_{th}^{out} a_{rfl}$. Then, the detailed outage probability analysis is presented as the following two theorems.

Theorem 1: We note that $P_{out,rfl}^{cl}(x) = 1$ when $a_{rfr} < \gamma_{th}^{SIC} a_{rfl}$. Under the case as $a_{rfr} > \gamma_{th}^{SIC} a_{rfl}$, we derive the closed-form outage probability expression of the reflecting user for the ES protocol as

$$P_{out,rfl}^{cl} = \sum_{n=0}^{\infty} \frac{4(-1)^n}{n!\sqrt{\pi}(2n+1)\left(2\eta_{eq}^{rfl}\right)^{\frac{2n+1}{2}}} \times \sum_{r=\{1,3,\cdots,2n+1\}}^{2n+1} \binom{2n+1}{r} \frac{R^{\frac{\alpha_t r}{2}}\left(\bar{h}_{eq}^{rfl}\right)^{2n+1-r}}{\frac{\alpha_t r}{2}+2} \times \left(\frac{\Upsilon_{\max} d_{BR}^{\alpha_t}}{P_t C_{BR} C_{RU}^{rfl}}\right)^{\frac{r}{2}}, \quad (17)$$

where $\Upsilon_{\max} = \max\left\{\frac{\gamma_{th}^{SIC}\sigma^2}{a_{rfr}-\gamma_{th}^{SIC}a_{rfl}}, \frac{\gamma_{th}^{out}\sigma^2}{a_{rfl}}\right\}$, γ_{th}^{out} is the outage threshold and $\binom{n}{r} = \frac{n!}{r!(n-r)!}$.

Proof: See Appendix B. ∎

Theorem 2: We note that $P_{out,rfr}^{cl}(x) = 1$ when $a_{rfr} < \gamma_{th}^{out} a_{rfl}$. Under the case as $a_{rfr} > \gamma_{th}^{out} a_{rfl}$ and with the aid of the ES protocol, the closed-form outage probability expression of the transmitting user is derived as

$$P_{out,rfr}^{cl} = \sum_{n=0}^{\infty} \frac{4(-1)^n}{n!\sqrt{\pi}(2n+1)\left(2\eta_{eq}^{rfr}\right)^{\frac{2n+1}{2}}} \times \sum_{r=\{1,3,\cdots,2n+1\}}^{2n+1} \binom{2n+1}{r} \frac{R^{\frac{\alpha_t r}{2}}\left(\bar{h}_{eq}^{rfr}\right)^{2n+1-r}}{\frac{\alpha_t r}{2}+2} \times \left(\frac{\Upsilon_2 d_{BR}^{\alpha_t}}{P_t C_{BR} C_{RU}^{rfr}}\right)^{\frac{r}{2}}, \quad (18)$$

where $\Upsilon_2 = \frac{\gamma_{th}^{out}\sigma^2}{a_{rfr}-\gamma_{th}^{out}a_{rfl}}$.

Proof: With the aid of (1) and the Taylor series of the error function, following the process of *Theorem 1*, this outage probability of the transmitting user can be derived as

$$P_{out,rfr}^{cl}(x) = \frac{2}{\sqrt{\pi}R^2}\int_0^R x\left(\sum_{n=0}^{\infty}\frac{(-1)^n}{n!(2n+1)}\Xi_1^{2n+1} - \frac{2}{\sqrt{\pi}}\sum_{n=0}^{\infty}\frac{(-1)^n}{n!(2n+1)}\Xi_2^{2n+1}\right)dx, \quad (19)$$

where $\Xi_1 = \frac{\bar{h}_{eq}^{rfr} + \sqrt{\frac{\Upsilon_2 d_{BR}^{\alpha_t} x^{\alpha_t}}{P_t C_{BR} C_{RU}^{rfr}}}}{\sqrt{2\eta_{eq}^{rfr}}}$, $\Xi_2 = \frac{\bar{h}_{eq}^{rfr} - \sqrt{\frac{\Upsilon_2 d_{BR}^{\alpha_t} x^{\alpha_t}}{P_t C_{BR} C_{RU}^{rfr}}}}{\sqrt{2\eta_{eq}^{rfr}}}$, and the theorem is proved by the binomial theorem. ∎

B. Curve Fitting Model

As the central limit theorem only fits the scenario when the RIS is large with plenties of RIS elements. For those with few RIS elements, the central limit model cannot match the simulation results well. Hence, we consider the curve fitting model to deal with this problem. We firstly note that

$P^{cf}_{out,rfl}(x) = 1$ when $a_{rfr} < \gamma^{SIC}_{th} a_{rfl}$ and $P^{cf}_{out,rfr}(x) = 1$ when $a_{rfr} < \gamma^{out}_{th} a_{rfl}$. Hence, we calculate the outage probability of the reflecting and transmitting users, respectively, when the outage probability is not constantly equal to one.

Theorem 3: We consider the scenario that all the channels through different RIS elements are independent. Based on the curve fitting model with the ES protocol, we model the RIS channel as an Gamma distribution. Under the case as $a_{rfr} > \gamma^{SIC}_{th} a_{rfl}$, we derive the closed-form outage probability expression of the reflecting user as

$$P^{cf}_{out,rfl} = \frac{2}{\Gamma(\alpha)} \sum_{n=0}^{\infty} \frac{(-1)^n R^{\alpha_t(\alpha+n)}}{n!(\alpha+n)[\alpha_t(\alpha+n)+2]} \times \left(\frac{\Upsilon_{\max} d^{\alpha_t}_{BR}}{P_t C_{BR} C^{rfl}_{RU} \beta_{rfl} \beta} \right)^{\alpha+n}. \quad (20)$$

Proof: See Appendix C. ∎

Theorem 4: We consider the same scenario in *Theorem 3*, that is, the independent channels among the RIS elements. Additionally, we consider the case $a_{rfr} > \gamma^{out}_{th} a_{rfl}$. Following the aforementioned constraints with the ES protocol, we derive the closed-form outage probability expression of the transmitting user as

$$P^{cf}_{out,rfr} = \frac{2}{\Gamma(\alpha) R^2} \sum_{n=0}^{\infty} \frac{(-1)^n}{n!(\alpha+n)} \left(\frac{\Upsilon_2 d^{\alpha_t}_{BR}}{P_t C_{BR} C^{rfr}_{RU} \beta_{rfr} \beta} \right)^{\alpha+n} \times \frac{R^{\alpha_t(\alpha+n)+2}}{[\alpha_t(\alpha+n)+2]}. \quad (21)$$

Proof: The proof is similar to the Appendix C. ∎

V. Numerical Results

The numerical coefficients setting can be defined as follows. The noise power is $\sigma^2 = -170 + 10\log(f_c) + N_f = -90$ dB, where the bandwidth f_c is 10 MHz and N_f is 10 dB. The transmit power P_t varies in $[10, 24]$ dBm. The path loss exponent is $\alpha_t = 2.4$. The thresholds are $\gamma^{SIC}_{th} = \gamma^{out}_{th} = 2^{0.1} - 1$. The power allocation coefficients are $a_{rfr} = 0.6$ and $a_{rfl} = 0.4$. The energy splitting coefficients are $\beta_{rfr} = 0.3$ and $\beta_{rfl} = 0.7$. The distance from the BS to RIS is $d_{BR} = 100$ m. The other coefficients are varied and specifically defined in the following paragraph. We denote "CL" as the central limit model and "CF" as the curve fitting model in the legends. In Fig. 2, we validate that the analytical channel models of STAR-RIS-aided users match numerical results well.

In Fig. 3, we further define the number of RIS elements as $M = \{20, 30\}$ and the radius of RIS deployment area as $R = 20$ m. Then, we investigate the outage performance versus the transmit SNR $\rho_t = P_t/\sigma^2$. One observation is that increasing the number of RIS elements can significantly increase the performance of NOMA users. In Fig. 4, the coefficients are defined that the number of RIS elements varies in $M = [10, 30]$ and the radius of RIS deployment area is chosen from $R = \{20, 30\}$ m. Hence, the outage performance versus the number of RIS elements is evaluated. we observe that reducing the RIS deployment range can enhance the performance as it reduces the influence of path loss.

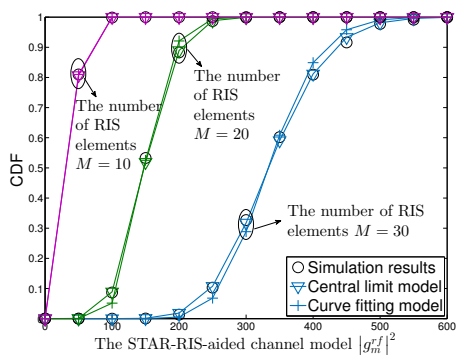

Fig. 2. CDF of the channel model with various numbers of RIS elements $M = \{10, 20, 30\}$.

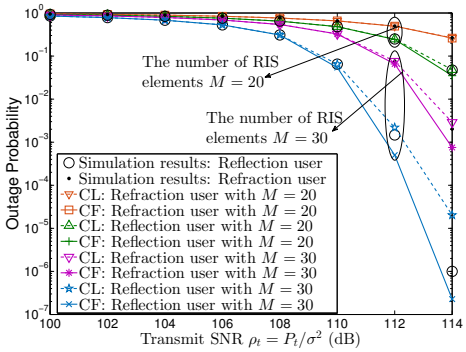

Fig. 3. Outage probability versus the transmit SNR with various numbers of RIS elements $M = \{20, 30\}$.

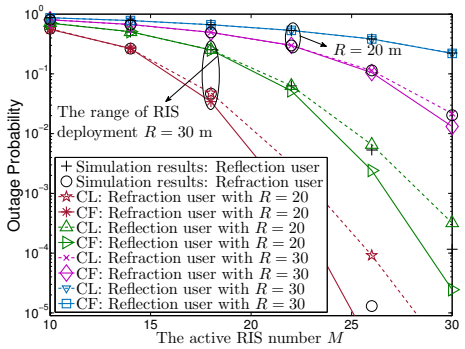

Fig. 4. Outage probability versus the number of RIS elements with various RIS deployment radii $R = \{20, 30\}$ m.

Comparing Fig. 3 and Fig. 4, we conclude that the two channel models match the low SNR regions better than the high SNR regions. Specifically, the curve fitting model performs as a lower bound of the simulation results while the central limit model is an upper bound.

VI. Conclusions

This paper has evaluated the outage probability of a STAR-RIS-aided downlink NOMA framework, where the NOMA users are randomly deployed in a circle area to capture the spatial effects of users. We have derived two STAR-RIS-aided channel models, namely the central limit model and the curve fitting model. The analytical results have revealed that 1) the central limit model has the closed-form expression as the items of error functions, and 2) the coefficients of the curve fitting model have the relationship with the number of RIS elements

as $\alpha = M$ and $\beta < M$. Based on the ES protocol, we have derived the closed-form expressions of outage probabilities for the transmitting and reflecting users, respectively. Numerical results have shown that: 1) STAR-RISs can enhance the channel quality of its aided user, 2) the two channel models perform as boundaries of the simulation results in high SNR regions, and 3) STAR-RISs can provide highly flexible decoding orders via adjusting the power splitting coefficient β_{rf}.

Appendix A: Proof of Lemma 1

As $\left|g_m^{rf}\right|^2 = \beta_{rf}\left(\sum_{m=1}^{M} h_{RU,m}^{rf} h_{BR,m}\right)^2$ for $rf \in \{rfl, rfr\}$, we exploit the central limit theorem to derive the variable $\left|g_m^{rf}\right| = \sqrt{\beta_{rf}}\left|\sum_{m=1}^{M} h_{RU,m}^{rf} h_{BR,m}\right|$. As we assume the independent Rician variables have the same mean and variance, denoted as $\bar{h}$ and η, we can derive the mean and variance of $\left|g_m^{rf}\right|$ as $\bar{h}_{eq}^{rf} = E\left(\left|g_m^{rf}\right|\right) = \sqrt{\beta_{rf}} M \bar{h}^2$ and $\eta_{eq}^{rf} = Var\left(\left|g_m^{rf}\right|\right) = \beta_{rf} M\left(2\bar{h}^2\eta + \eta^2\right)$, where $E(\cdot)$ and $Var(\cdot)$ are the expectation and variance of a certain variable.

Hence, we can express the PDF of $\left|g_m^{rf}\right|$ as

$$f_{\left|g_m^{rf}\right|}(x) = \frac{1}{\sqrt{2\pi\eta_{eq}^{rf}}} \exp\left(-\frac{\left(x - \bar{h}_{eq}^{rf}\right)^2}{2\eta_{eq}^{rf}}\right). \tag{A.1}$$

Based on the derivation for a variable x that $f_{x^2}(y) = \frac{1}{2\sqrt{y}}\left(f_x\left(\sqrt{y}\right) + f_x\left(-\sqrt{y}\right)\right)$, we derive the PDF of $\left|g_m^{rf}\right|^2$ as

$$f_{\left|g_m^{rf}\right|^2}(y) = \frac{1}{2\sqrt{2\pi\eta_{eq}^{rf} y}}\left(\exp\left(-\frac{\left(\sqrt{y} - \bar{h}_{eq}^{rf}\right)^2}{2\eta_{eq}^{rf}}\right) + \exp\left(-\frac{\left(\sqrt{y} + \bar{h}_{eq}^{rf}\right)^2}{2\eta_{eq}^{rf}}\right)\right). \tag{A.2}$$

Then, we can derive the CDF of the channel model as *Lemma 1* according to the derivation as $\int_0^x \frac{1}{\sqrt{y}}\left(\exp\left(-\frac{\left(\sqrt{y}-a\right)^2}{b}\right) + \exp\left(-\frac{\left(\sqrt{y}+a\right)^2}{b}\right)\right) dy = \sqrt{\pi b} \times \left(\operatorname{erf}\left(\frac{a+\sqrt{x}}{\sqrt{b}}\right) - \operatorname{erf}\left(\frac{a-\sqrt{x}}{\sqrt{b}}\right)\right)$.

Appendix B: Proof of Theorem 1

With the aid of the outage probability definition, the outage probability of the reflecting user can be expressed as

$$P_{out,rfl}^{cl}(x) = \int_0^R F_{\left|g_m^{rfl}\right|^2}\left(\frac{\Upsilon_{\max} d_{BR}^{\alpha_t} x^{\alpha_t}}{P_t C_{BR} C_{RU}^{rfl}}\right) f_{d_{RU}^{rfl}}(x)\, dx. \tag{B.1}$$

Substituting the CDF of the central limit model and (1) into (B.1), we can further derive the expression above as

$$P_{out,rfl}^{cl}(x) = \int_0^R \frac{x}{R^2}\left(\operatorname{erf}(\Xi_3) - \operatorname{erf}(\Xi_4)\right) dx, \tag{B.2}$$

where $\Xi_3 = \frac{\bar{h}_{eq}^{rfl} + \sqrt{\frac{\Upsilon_{\max} d_{BR}^{\alpha_t} x^{\alpha_t}}{P_t C_{BR} C_{RU}^{rfl}}}}{\sqrt{2\eta_{eq}^{rf}}}$ and $\Xi_4 = \frac{\bar{h}_{eq}^{rfl} - \sqrt{\frac{\Upsilon_{\max} d_{BR}^{\alpha_t} x^{\alpha_t}}{P_t C_{BR} C_{RU}^{rfl}}}}{\sqrt{2\eta_{eq}^{rf}}}$.

As the integration above cannot be derived, we utilize the Taylor series of the error function $\operatorname{erf}(z) = \frac{2}{\sqrt{\pi}}\sum_{n=0}^{\infty}\frac{(-1)^n}{n!(2n+1)} z^{2n+1}$ to approximately calculate the outage probability. Hence, we derive the equation (B.2) as

$$P_{out,rfl}^{cl}(x) = \sum_{n=0}^{\infty} \frac{4(-1)^n}{n!\sqrt{\pi}(2n+1)\left(2\eta_{eq}^{rfl}\right)^{\frac{2n+1}{2}}} \times \sum_{r=\{1,3,\cdots,2n+1\}}^{2n+1} \binom{2n+1}{r} \times \left(\bar{h}_{eq}^{rfl}\right)^{2n+1-r}\left(\frac{\Upsilon_{\max} d_{BR}^{\alpha_t}}{P_t C_{BR} C_{RU}^{rfl}}\right)^{\frac{r}{2}} \int_0^R \frac{x^{\frac{\alpha_t r}{2}+1}}{R^2} dx, \tag{B.3}$$

and after calculating the integration $\int_0^R \frac{x^{\frac{\alpha_t r}{2}+1}}{R^2} dx = \frac{R^{\frac{\alpha_t r}{2}}}{\frac{\alpha_t r}{2}+2}$, we can obtain the final expressions.

Appendix C: Proof of Theorem 3

Firstly, we substitute the CDF of the Gamma distribution, (13), into the definition of the outage probability of the reflecting user, (15). Hence, we can obtain the integration as

$$P_{out,rfl}^{cf}(x) = \frac{2}{\Gamma(\alpha) R^2}\int_0^R x\gamma\left(\alpha, \frac{\Upsilon_{\max} d_{BR}^{\alpha_t} x^{\alpha_t}}{P_t C_{BR} C_{RU}^{rfl} \beta_{rfl} \beta}\right) dx. \tag{C.1}$$

We then exploit the Taylor series the expand the incomplete Gamma function as $\gamma(\alpha, \beta) = \sum_{n=0}^{\infty}\frac{(-1)^n \beta^{\alpha+n}}{n!(\alpha+n)}$. In this way, we can further calculate the equation above as the following

$$P_{out,rfl}^{cf}(x) = \frac{2}{\Gamma(\alpha) R^2}\sum_{n=0}^{\infty}\frac{(-1)^n}{n!(\alpha+n)} \times \left(\frac{\Upsilon_{\max} d_{BR}^{\alpha_t}}{P_t C_{BR} C_{RU}^{rfl} \beta_{rfl} \beta}\right)^{\alpha+n} \int_0^R x^{\alpha_t(\alpha+n)+1} dx. \tag{C.2}$$

Finally, we obtain the final answers by deriving the integration $\int_0^R x^{\alpha_t(\alpha+n)+1} dx = \frac{R^{\alpha_t(\alpha+n)+2}}{[\alpha_t(\alpha+n)+2]}$.

References

[1] S. Zeng, H. Zhang, B. Di, Y. Tan, Z. Han, H. Vincent Poor, and L. Song, "Reconfigurable intelligent surfaces in 6G: Reflective, transmissive, or both?" *IEEE Commun. Lett.*, pp. 1–1, 2021.

[2] Q. Wu and R. Zhang, "Towards smart and reconfigurable environment: Intelligent reflecting surface aided wireless network," *IEEE Commun. Mag.*, vol. 58, no. 1, pp. 106–112, 2020.

[3] J. Xu, Y. Liu, X. Mu, and O. A. Dobre, "SRAR-RISs: Simultaneous reflecting and refracting reconfigurable intelligent surfaces," *arXiv preprint arXiv:2101.09663*, 2021.

[4] X. Mu, Y. Liu, L. Guo, J. Lin, and R. Schober, "Simultaneously transmitting and reflecting (STAR) RIS aided wireless communications," *arXiv preprint arXiv:2104.01421*, 2021.

[5] S. Zhang, H. Zhang, B. Di, Y. Tan, Z. Han, and L. Song, "Beyond intelligent reflecting surfaces: Reflective-transmissive metasurface aided communications for full-dimensional coverage extension," *arXiv preprint arXiv:2009.06878*, 2020.

[6] S. Zhang, H. Zhang, B. Di, Y. Tan, M. Di Renzo, Z. Han, H. Vincent Poor, and L. Song, "Intelligent omni-surface: Ubiquitous wireless transmission by reflective-transmissive metasurface," *arXiv preprint arXiv:2011.00765*, 2020.

[7] Y. Liu, X. Mu, J. Xu, R. Schober, Y. Hao, H. Vincent Poor, and L. Hanzo, "STAR: Simultaneous transmission and reflection for 360° coverage by intelligent surfaces," *arXiv preprint arXiv:2103.09104*, 2021.